# Close-Packed Noncircular Nanodevice Pattern Generation by Self-Limiting Ion-Mill Process

**Vishal A. Parekh,[†] Ariel Ruiz,[†] Paul Ruchhoeft,[†] Stanko Brankovic,[†] and Dmitri Litvinov*,[†,‡]**

*Electrical and Computer Engineering, University of Houston, Houston, Texas 77204, and Chemical & Biomolecular Engineering, University of Houston, Houston, Texas 77204*

## ABSTRACT

We describe a self-limiting, low-energy argon-ion-milling process that enables noncircular device patterns, such as squares or hexagons, to be formed using precursor arrays of uniform circular openings in poly(methyl methacrylate) defined using electron beam lithography. The proposed patterning technique is of particular interest for bit-patterned magnetic recording medium fabrication, where square magnetic bits result in improved recording system performance. Bit-patterned magnetic medium is among the primary candidates for the next generation magnetic recording technologies and is expected to extend the areal bit density limits far beyond 1 Tbit/in$^2$. The proposed patterning technology can be applied either for direct medium prototyping or for manufacturing of nanoimprint lithography templates or ion beam lithography stencil masks that can be utilized in mass production.

Conventional magnetic recording based on writing data into *continuous* polycrystalline medium is rapidly approaching its superparamagnetic areal bit density limit of ∼500 Gbits/in.$^2$.[1,2] The inherent randomness of polycrystalline continuous media requires each bit to pack a relatively large number of magnetically semi-independent grains (∼60−100) to enable practical signal-to-noise ratios. In turn, the grain size approximately defines the thermal activation volume and, thus, defines the smallest thermally stable bit size. Bit patterning allows for a significant reduction in the number of magnetically independent grains per bit to the one-grain-per-bit limit, thus allowing for higher bit densities. It is expected to extend the achievable areal bit density limits beyond 1 Tbit/in.$^2$.[3−5] The key, however, to technology commercialization remains the development of a cost-effective fabrication strategy.

Nanoimprint lithography[6−8] and ion beam proximity lithography (IBPL)[9−11] have been actively explored for bit-patterned medium fabrication. In IBPL, a stencil mask (a membrane with etched openings) is illuminated by a broad beam of energetic helium ions, and the ions pass through the openings replicating the entire mask pattern in the resist in a single exposure. The resolution limit of this technique is primarily imposed by system blur (penumbral blur due to a finite source size) and ion scattering within the resist[12,13]

and is expected to be on the scale of a few nanometers. The penumbral blur depends on the angular extent of the source and the distance between the stencil mask and the substrate, and using a small (e.g., 10 $\mu$m) mask-to-wafer gap thus overcomes the practical limitations of diffraction and penumbra. Moreover, electrostatic deflection of the ion beam can be used to change the incident angle of the beam and, in such, form multiple offset images, and is the basis of aperture array lithography.[9]

Both IBPL and imprint lithography require high-resolution e-beam lithography for generating master-beam-shaping stencil masks and imprint stamps, respectively. Unfortunately, periodic close packed noncircular device patterns (square bits in bit-patterned media help optimize the recording system performance) with sub-100-nm critical dimensions are difficult to define using e-beam lithography due to proximity effects, especially if high spatial resolution corners are required. Here we present a novel technique for defining patterns containing closely packed squares and hexagons using a simple-to-generate by e-beam lithography precursor pattern in poly(methyl methacrylate) (PMMA) resist, stencil mask fabrication being chosen as an illustrative example.

The stencil mask fabrication process starts with the fabrication of a silicon nitride membrane[14] followed by a palladium hard mask layer sputter deposited onto the membrane. The key challenge is to form the desired device pattern in the Pd layer, which is used as a pattern transfer

* Corresponding author. E-mail: dlitvinov@uh.edu.
† Electrical and Computer Engineering.
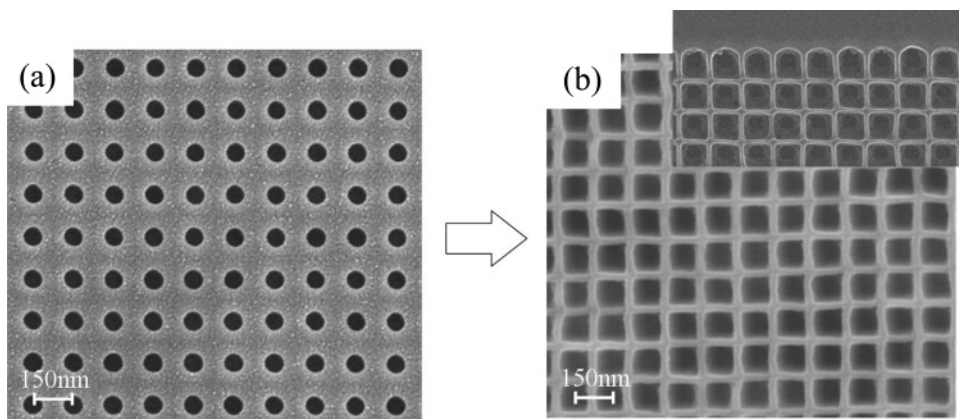‡ Chemical & Biomolecular Engineering.

**Figure 1.** (a) A SEM image of ~75 nm openings on a square grid formed in PMMA using e-beam lithography. (b) Top view of 107 nm square openings on a 150 nm pitch after 12 min of self-limiting $Ar^+$ ion milling at a beam energy of 500 eV. The insert shows the edge of the pattern where the self-limiting process fails.
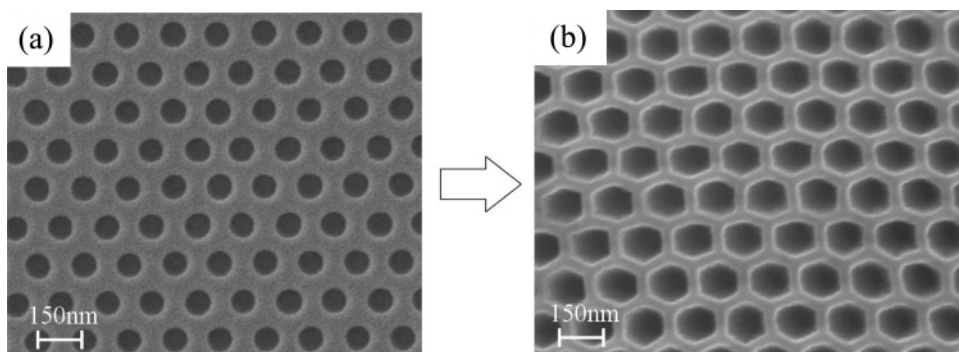


**Figure 2.** (a) An SEM image of ~85 nm openings (with $\sigma = 2.0$ nm) on a hexagonal grid formed in PMMA using e-beam lithography. (b) Top view of 105 nm (with $\sigma = 3.0$ nm) hexagonal openings on a 150 nm pitch after 12 min of self-limiting $Ar^+$ ion milling at a beam energy of 500 eV.

layer into silicon nitride membrane by selective highly anisotropic $CF_4/O_2$ reactive ion etching. A 600 nm PMMA resist coating is then spun onto a 20 nm thick Pd layer, and ~75 nm average diameter circular openings (with $\sigma = 1.8$ nm in the diameter) on a 150 nm pitch were patterned in PMMA using e-beam lithography as shown in Figure 1a. Argon ion milling using a Veeco RF ion source was then carried out for 12 min at a base pressure of $4 \times 10^{-6}$ Torr and a gas pressure of 0.4 mTorr, with a beam energy of 500 eV and a discharge power of 50 W. The resulting structures are shown in Figure 1b, where the initial circular openings have transformed into a lattice of 107 nm average diameter squares with $\sigma = 3.8$ nm. Significantly, the square morphology breaks down at the edges of the pattern as illustrated in the insert in Figure 1b, where the circular structure continues to expand away from the array.

The square patterns are formed by a self-limiting process where the PMMA erosion rate is drastically reduced after reaching a critical wall thickness. In this way, the openings become larger, with their circular shape retained, until the etching slows when the thickness of the wall, which is formed with the adjacent openings, reaches a critical thickness. The regions where the wall is still thicker (e.g., in the direction of the diagonal) continues to thin more rapidly until a square opening forms when the thickness of the walls is uniform. Similar behavior is seen for diagonally placed

structures, as shown in Figure 2, which become high spatial resolution honeycomb structures.

This behavior is attributed to a depletion of reactive compounds from within the bulk of the resist as the wall thins. PMMA that is bombarded by the low-energy ions forms a thin carbon-rich polymer, mainly α-C−H ($sp^3$ hybridization) and α-C ($sp^2$ hybridization), that has an inherently lower sputter yield.[15] The thickness of this carbon-rich layer is estimated to be 8−10 nm for an $Ar^+$ ion beam energy of 500 eV. Removal rates of the surface remain relatively high as reactive gases are freed from within the polymer bulk and diffuse to the surface forming volatile compounds. However, the etch rate drops drastically (by at least a factor of 4[16]) when the PMMA wall thickness approaches twice the thickness of the carbon-rich layer in this case. In our experiments, the wall thickness between the squares reduced to 25 nm after 7 min of etching, and further etching for 5 min did not change the wall thickness considerably.

The $Ar^+$ ions penetrating deeper into PMMA beyond the graphitized layer induce radiation-chemical reaction leading to desorption of gases from PMMA. The etch rate of the top surface of PMMA is therefore determined by not only the sputter rates of graphitized layer but also the gases leaching from the subsurface PMMA.[15] As applied to square pattern formation, the lateral etching of the circular opening
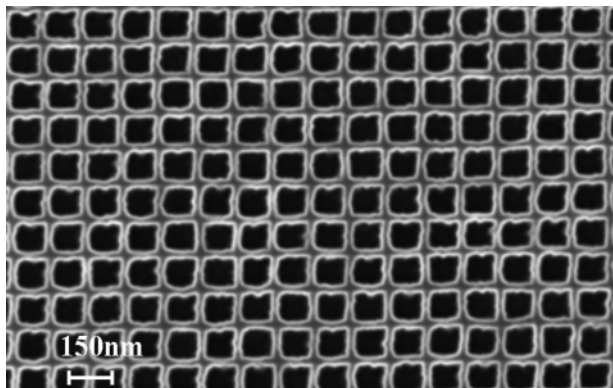
**Figure 3.** SEM image of square openings transferred into Pd hard mask by Ar ion milling.

side walls (due to nonperfect collimation of the ion mill used in this work) results in the widening of the circular openings and the thinning of the wall separating the circles. Once the thickness of the wall reaches a critical thickness, which is equal to approximately twice the graphitized layer thickness, the lateral etch rate significantly reduces, thus forming sharp corners in the pattern (squares).

The self-limiting process for square and hexagon formation strongly depends on the diameter and the pitch of the circular openings in PMMA. It was determined that in order to observe this effect, the pitch should be ∼1.5−2 times the diameter of the circular openings. A pitch greater than 2× leaves a significant amount of material to be etched laterally requiring a much longer over-etch time, an increased PMMA layer thickness, and decreased fidelity of the resulting pattern.

The square matrix of graphitized PMMA was transferred into underlying Pd layer using further argon ion milling. A scanning electron microscopy (SEM) image of resultant square pattern in Pd layer is shown in Figure 3.

In summary, we have demonstrated a self-limiting argon ion milling process that enables the formation of high spatial resolution square or hexagonal device patterns in PMMA. The process has been optimized for IBPL stencil mask fabrication but can be applied elsewhere where close-packed noncircular device patterns are of interest and which are difficult to achieve using e-beam lithography. Furthermore, the proposed process is expected to be scalable into the deep sub-100-nm scale as the thickness of the graphitized PMMA layer and the milling rates can be effectively controlled by ion mill beam parameters such as energy, current density,

etc. In addition to applications in patterned medium, the proposed technology can be applied in various other areas of nanotechnology including fabrication of high-density semiconductor memories, infrared filters,[17] filtration membranes,[18] etc.

## References

(1) Charap, S. H.; Lu, P. L.; He, Y. J. *IEEE Trans. Magn.* **1997**, *33* (1), 978−983.
(2) Bertram, H. N.; Williams, M. *IEEE Trans. Magn.* **2000**, *36* (1), 4−9.
(3) Hughes, G. F. *IEEE Trans. Magn.* **2000**, *36* (2), 521−527.
(4) Rettner, C. T.; Best, M. E.; Terris, B. D. *IEEE Trans. Magn.* **2001**, *37* (4), 1649−1651.
(5) Ross, C. *Annu. Rev. Mater. Res.* **2001**, *31*, 203−235.
(6) Mancini, D. P.; Resnick, D. J.; Sreenivasan, S. V.; Watts, M. P. C. *Solid State Technol.* **2004**, *47* (2), 55−+.
(7) Chou, S. Y.; Krauss, P. R.; Zhang, W.; Guo, L. J.; Zhuang, L. *J. Vacuum Sci. Technol., B* **1997**, *15* (6), 2897−2904.
(8) Ruchhoeft, P.; Colburn, M.; Choi, B.; Nounu, H.; Johnson, S.; Bailey, T.; Damle, S.; Stewart, M.; Ekerdt, J.; Sreenivasan, S. V.; Wolfe, J. C.; Willson, C. G. *J. Vacuum Sci. Technol., B* **1999**, *17* (6), 2965−2969.
(9) Ruchhoeft, P.; Wolfe, J. C. *J. Vacuum Sci. Technol., B* **2001**, *19* (6), 2529−2532.
(10) Wolfe, J. C.; Pendharkar, S. V.; Ruchhoeft, P.; Sen, S.; Morgan, M. D.; Horne, W. E.; Tiberio, R. C.; Randall, J. N. *J. Vacuum Sci. Technol., B* **1996**, *14* (6), 3896−3899.
(11) Parekh, V.; Chunsheng, E.; Smith, D.; Ruiz, A.; Wolfe, J. C.; Ruchhoeft, P.; Svedberg, E.; Khizroev, S.; Litvinov, D. *Nanotechnology* **2006**, *17* (9), 2079−2082.
(12) Kaesmaier, R.; Loschner, H.; Stengl, G.; Wolfe, J. C.; Ruchhoeft, P. *J. Vacuum Sci. Technol., B* **1999**, *17* (6), 3091−3097.
(13) Ruchhoeft, P.; Wolfe, J. C. *J. Vacuum Sci. Technol., B* **2000**, *18* (6), 3177−3180.
(14) Han, K. Fabrication of Micro-Filtration Membranes Using Ion Beam Aperture Array Lithography. University of Houston, Houston, 2004.
(15) Koval, Y. *J. Vacuum Sci. Technol., B* **2004**, *22* (2), 843−851.
(16) Gokan, H.; Esho, S.; Ohnishi, Y. *J. Electrochem. Soc.* **1983**, *130* (1), 143−6.
(17) Qiang, R.; Chen, J.; Zhao, T. X.; Han, K. P.; Ruiz, A.; Ruchhoeft, P.; Morgan, M. *Microwave Opt. Technol. Lett.* **2006**, *48* (9), 1749−1754.
(18) Han, K. P.; Xu, W. D.; Ruiz, A.; Ruchhoeft, P.; Chellam, S. *J. Membr. Sci.* **2005**, *249* (1−2), 193−206.

NL071793R